Using Variable Frequency Asymmetries to Understand Radial Transport in a Malmberg-Penning Trap

D.L. Eggleston

Occidental College, Physics Department, Los Angeles, California 90041

Abstract. It has long been known that asymmetric electric and magnetic fields produce radial transport in Malmberg-Penning traps, and much work has been done to understand this transport. Our approach is to apply a variable frequency electric asymmetry to a low density population of electrons and to measure the resulting radial particle flux Γ as a function of radius r. The low particle density eliminates many plasma modes (which have their own frequency dependence) and allows us to focus on the transport physics. The usual azimuthal $E \times B$ drift is maintained by a biased central wire, and this arrangement also allows us to independently vary the drift frequency ω_R by adjusting either the axial magnetic field B_z or the bias of the central wire ϕ_{cw}. Up to forty wall sectors are used in order to apply an asymmetry consisting of a single fourier mode (n, l, ω), where n is the axial wavenumber, l is the azimuthal wavenumber, and ω is the asymmetry frequency. In the current experiments, we vary ω, n, ϕ_{cw}, and B_z. As ω is varied, the particle flux shows a resonance similar to that predicted by resonant particle theory. The peak frequency of this resonance f_{peak} increases with ω_R and varies with n, in qualitative agreement with theory, but when quantitative comparisons are made the experimental values for f_{peak} do not match those predicted by theory. Instead, the dependence of f_{peak} on ϕ_{cw}, B_z, and r follows simple empirical scaling laws: for inward directed flux, $f_{peak}(\mathrm{MHz}) \approx |-R\phi_{cw}(\mathrm{V})/rB_z(\mathrm{G})|^{1/2}$, where R is the wall radius, and for outward directed flux, $f_{peak}(\mathrm{MHz}) \approx 0.8|-\phi_{cw}(\mathrm{V})/B_z(\mathrm{G})|^{1/2}$. These results may provide guidance for the construction of the correct theory of asymmetry-induced transport.

INTRODUCTION

It has been known for some time that the confinement in Malmberg-Penning traps is limited by the presence of electric or magnetic fields that break the cylindrical symmetry of the trap. Such asymmetries produce a radial component to the $E \times B$ or grad-B drift that leads to particle loss. This basic understanding is supported by confinement studies [1, 2] as well as experiments with applied electric [3, 4, 5, 6, 7, 8] and magnetic [9, 10] asymmetries.

Many of these early papers also suggested that this asymmetry-induced transport might be described by a theoretical model developed for studies of radial transport in the early tandem mirrors (see, e.g., [11, 12]) where static, asymmetric end cells produced radial grad-B drifts that largely determined the radial particle flux. A key prediction of the theory is that the resulting transport will be dominated by particles whose axial bounce motion and azimuthal drift motion causes them to move in resonance with the asymmetry. As these resonant particles repeatedly encounter the asymmetry they take radial steps in the same direction, thus allowing them to diffuse more quickly than non-

CP692, *Non-Neutral Plasma Physics V*, edited by M. Schauer et al.

resonant particles.

Here we present experiments that test this key prediction of the theory. We do this by applying a variable frequency electrostatic asymmetry to a Malmberg-Penning trap and measuring the resulting radial particle transport as a function of the asymmetry frequency. Our modified trap design avoids previously encountered complications produced by collective effects and allows for a clean test of the transport physics. While the experimental results are qualitatively consistent with theory and seem to confirm the dominant role played by resonant particles, the frequency dependence of the transport does not quantitatively match the predictions of theory.

ASYMMETRY-INDUCED TRANSPORT THEORY AND EXPERIMENTAL APPROACH

Our experiments are performed in a modified Malmberg-Penning trap in which the plasma has been replaced by a biased wire and the transport of low density test particles is studied. This experimental approach is best understood in the context of asymmetry-induced transport theory, so we begin with a summary of the theory as recently adapted to Malmberg-Penning traps and allowing for electric field asymmetries at a non-zero angular frequency ω [13]. The theory assumes a cylindrical geometry with an axial magnetic field B_z. Asymmetric electric fields are applied by placing voltages on wall sectors. Under these conditions, the resulting radial particle flux for the plateau regime (suitable for small asymmetry amplitudes) is given by (see reference [13] for details)

$$\Gamma_{plateau} = -\sum_{n,l,\omega} \frac{n_0}{\sqrt{2\pi\overline{v}^2}} \frac{L}{|n|} \left| \frac{cl\phi_{nl\omega}(r)}{rB_z} \right|^2 \left[\frac{1}{n_0}\frac{dn_0}{dr} + \sqrt{2}\frac{n\pi}{L}\frac{r\omega_c}{l\overline{v}}x \right] e^{-x^2}. \qquad (1)$$

Here $\phi_{nl\omega}(r)$ is the Fourier amplitude of the asymmetry mode characterized by axial mode n, azimuthal mode l, and angular frequency ω. For simplicity, we have assumed here that the temperature T is constant with radius. The variable x is equal to $v_{res}/\sqrt{2}\overline{v}$, where

$$v_{res} = \frac{L}{n\pi}(\omega - l\omega_R) \qquad (2)$$

is the resonant velocity for the asymmetry mode n, l, ω and ω_R is the azimuthal $E \times B$ rotation frequency of the plasma column. The symbols n_0, L, $\overline{v}$, and ω_c denote the electron density, plasma length, thermal velocity, and the cyclotron frequency, respectively.

It is worth noting several features of Eq. (1). The radial flux involves a sum over all the asymmetry modes produced by the wall voltages. The square brackets contain a diffusive term $\frac{1}{n_0}\frac{dn_0}{dr}$ and a generalized mobility $\sqrt{2}\frac{n\pi}{L}\frac{r\omega_c}{l\overline{v}}x$ (note that this latter term reduces to eE/kT for $\omega = 0$). The plateau regime flux is proportional to the square of the asymmetry amplitude $\phi^2_{nl\omega}$. Our previous studies of the amplitude scaling [8] of this transport suggest that we are in the plateau regime, but the results of this paper are not dependent upon that identification because both the plateau regime and the banana regime suitable for higher asymmetry amplitudes have the same frequency dependence. The previously mentioned domination of the transport by resonant particles is reflected

in the e^{-x^2} factor, which stems from evaluating the Maxwellian distribution function at the resonant velocity. Note that x can be positive or negative since ω may be greater than or less than ω_R. Here, we use the convention that $\omega > 0$ corresponds to an asymmetry that rotates with the plasma column and $\omega < 0$ corresponds to one that rotates against the column. When the second term in brackets dominates over the first, a static field asymmetry ($\omega = 0, x < 0$) will move electrons radially outward ($\Gamma > 0$), but an appropriately chosen asymmetry ($\omega > \omega_R, x > 0$) can move particles radially inward. Such inward transport has been observed in "rotating wall" experiments [3, 5, 14, 15, 16].

The presence of ω in the variable x provides the experimentalist with an ideal way of testing the notion that resonant particles dominate the transport. By varying ω, one can obtain any value of the resonant velocity v_{res} (see Eq. (2)) while keeping other experimental parameters fixed. The resulting radial flux should then exhibit a resonance as v_{res} sweeps through the distribution function. The ability to place v_{res} in the bulk of the distribution function also makes it possible to obtain a measurable amount of radial transport while keeping the asymmetry amplitude low. This approach, however, is complicated by the strong ω-dependence of the asymmetry potential $\phi_{nl\omega}(r)$ in the plasma. Numerical studies for typical plasma parameters [13] show that the transport-producing electric field in the plasma (i.e. $E_\theta = l\phi_{nl\omega}/r$) can vary by many orders of magnitude as adjustments of ω produce plasma phenomena ranging from standing waves to Debye shielding. These variations in E_θ (and thus in the radial flux Γ) tend to dominate or mask those produced by resonant particle effects. This produces, for example, enhanced transport when the asymmetry drives a helical standing wave of the plasma column as was observed in previous experiments [3, 14, 15, 16]. While these collective processes are interesting, they are not essential to the transport physics. In this context we note that these numerical studies also show that the variations of E_θ with ω can be reduced as the temperature is increased or the density is reduced.

These considerations led us to employ the modified trap design shown in Fig. 1. The axial magnetic field and negatively biased end cylinders of the standard trap design are retained, but the plasma is replaced by a thin biased wire (0.356 mm diam.) suspended along the axis of the trap. This wire provides a radial electric field to replace the field normally produced by the plasma column and allows low density electrons injected into this device to have the same zeroth-order dynamical motions as those in a typical non-neutral plasma (axial bounce and azimuthal $E \times B$ drift motions). The collective variations of $\phi_{nl\omega}(r)$, however, are minimized since the lower density (10^5 cm^{-3}) and higher temperature (4 eV) of the electrons give a Debye length (λ_D = 4.7 cm) larger than the trap radius (R = 3.82 cm). Under these conditions, the applied asymmetry potentials are essentially the vacuum potentials and their ω-dependence is eliminated. In short, we have constructed a trap where the electrons will act as test particles moving in the prescribed fields. Despite these changes, the confinement time scaling with no applied asymmetries [17] shows the same $(L/B_z)^2$ dependence found in higher density experiments [1, 2], supporting the notion that the radial transport is primarily a single particle effect.

Experiments studying asymmetry-induced transport typically use azimuthally sectored cylinders in the confinement region to apply asymmetric electric fields. In our device, we have sectored the entire confinement region (five cylinders, labeled S1 through

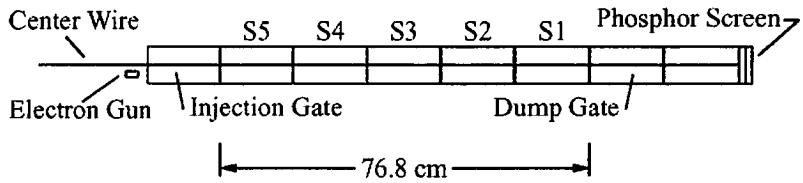

FIGURE 1. Schematic of the Occidental Trap. The usual plasma column is replaced by a biased wire that maintains the basic dynamical motions of low density electrons injected from an off-axis gun. The low density and high temperature of the injected electrons largely eliminates collective modifications of the vacuum asymmetry potential. The five cylinders labeled S1 through S5 are divided azimuthally into eight sectors. These forty wall sectors allow for the application of asymmetries consisting of essentially one Fourier mode.

S5 in Fig. 1, with eight azimuthal divisions each), for two reasons. The first reason is to ensure that the applied potentials stay small enough for the theory to be valid. When the potential ϕ_W is applied on a single sector of length L_s, the amplitude of the Fourier modes will be proportional to $(L_s/L)\phi_W$, where L is the length of the plasma. The smaller L_s/L is, the larger the wall potential necessary to produce a mode $\phi_{nl\omega}$ of given amplitude and thus a given amount of transport. The amplitude of the wall potential, however, is not unrestricted: linear theory assumes the trajectories of the electrons are not radically different from the unperturbed case, and thus requires $e\phi_W << kT_e$. In order to satisfy the theoretical assumptions while producing an observable amount of transport, it is thus advantageous to sector the entire confinement region.

The second reason for our modifications to the confinement region is to allow a clean, unambiguous test of theory. As previously noted, the theoretical expressions for the radial flux involve a sum over Fourier modes n, l, and ω, with each mode contributing to the total transport. Experimental measurement of the flux, however, produces a single number Γ. Comparison to a theoretical expression that involves a sum over terms will therefore always be somewhat ambiguous since the combination of terms producing a given flux value is not unique. The least ambiguous case would involve a single Fourier mode, but this requires many wall sectors. Forty sectors is a number that can be reasonably handled and represents a great improvement over previous experiments. By judiciously selecting the amplitude and phase of the signals applied to each sector, we can produce an asymmetry that is essentially a single Fourier mode, with higher harmonics typically having amplitudes smaller than 10% of this mode's. For these experiments, we used a helical standing wave of the approximate form

$$\phi(r,\theta,z,t) = \phi_W \frac{r}{R} cos\left(\frac{n\pi z}{L}\right) cos(l\theta - \omega t) \tag{3}$$

where ϕ_W is the asymmetry potential at the wall (typically 0.2 V), R is the wall radius (3.82 cm), L is the length of the confinement region (76.8 cm), and z is measured from one end of the confinement region. This asymmetry, which decomposes into oppositely propagating helical modes, will allow particles to maintain resonance with the asymmetry when they bounce off the ends of the trap and change direction. For most of this work, the wall sectors are configured to give an asymmetry where the $n = 1, l = 1$ mode is dominant. By adjusting the relative phase of the applied signals, the asymmetry

can be made to rotate either with the zeroth-order azimuthal drift ($\omega > 0$) or against it ($\omega < 0$).

With the frequency dependence of $\phi_{nl\omega}(r)$ eliminated by increasing the Debye length and the sum over modes removed by the strategic use of multiple wall sectors, the expression for the flux can be simplified to

$$\Gamma = -C\,[A + Bx]\,e^{-x^2} \tag{4}$$

where $A = dn_0/dr$, $B = \sqrt{2}n_0 r\omega_c n\pi/(l\overline{v}L)$, and C contains the remaining factors in Eq. (1). The remaining frequency dependence is contained in the normalized resonance velocity x. As the asymmetry frequency is varied, the flux will have extrema when $d\Gamma/dx = 0$. Applying this to Eq.(4) and solving for x gives

$$x_{peak} = \frac{1}{2}\left[-\frac{A}{B} \pm \sqrt{\left(\frac{A}{B}\right)^2 + 2}\right] \tag{5}$$

or

$$\omega_{peak} = l\omega_R + \frac{\sqrt{2}}{2}\frac{n\pi}{L}\overline{v}\left[-\frac{A}{B} \pm \sqrt{\left(\frac{A}{B}\right)^2 + 2}\right] \tag{6}$$

Note that the solutions for x_{peak} depend only on the ratio A/B. The two solutions correspond to two flux peaks of opposite signs, with the plus sign corresponding to flux minima and the minus sign corresponding to flux maxima. Because of the Gaussian dependence on x in Eq. (4), often only one of these peaks will be sizable.

The remaining features of the trap have been discussed in detail elsewhere [17, 18]. Electrons injected into the trap from an off-axis gun are quickly dispersed into an annular distribution. At a chosen time (here, 1600 ms after injection), the asymmetries are switched on for a period of time δt (here, 100 ms) and then switched off. At the end of the experiment cycle, the electrons are dumped axially onto a phosphor screen and the resulting image is digitized using a 512×512 pixel charge-coupled device camera. A radial cut through this image gives the density profile $n_0(r)$ of the electrons, where calibration is provided by a measurement of the total charge being dumped. Profiles are taken both with the asymmetry on and off, and the resulting change in density $\delta n_0(r)$ is obtained. If the asymmetry amplitude is small enough and the asymmetry pulse length δt short enough, then $\delta n_0(r)$ will increase linearly in time. We may then approximate $dn_0/dt \simeq \delta n_0(r)/\delta t$ and calculate the radial particle flux $\Gamma(r)$ (assuming $\Gamma(r = a) = 0$):

$$\Gamma(r) = -\frac{1}{r}\int_a^r r'dr' \cdot \frac{dn_0}{dt}(r') \tag{7}$$

Here a is the radius of the central wire. The entire experiment is then repeated for a series of asymmetry frequencies and the resulting flux vs. radius and frequency data saved for analysis.

EXPERIMENTAL RESULTS

A typical result is shown in Fig. 2 where we plot the radial flux Γ vs. asymmetry frequency f for four selected radii. The radial density profile is shown in the inset. There are several things to note in this figure. First, note that the predominant flux peaks occur only for positive frequencies. This is in marked contrast to other experiments [3, 14, 15, 16] where driven plasma modes (which occur for both positive and negative frequencies) dominated the transport and produced flux peaks for both positive and negative frequencies. The data thus supports the conclusion that we have effectively limited the role of collective modes in the experiment. Second, the fact that the flux peaks occur only for positive frequencies is in qualitative agreement with the theory. As Eq. (4) shows, the frequency dependence of the theoretical flux is constrained by the factor e^{-x^2}, a Gaussian curve centered where $\omega = l\omega_R$. Since ω_R is a positive quantity and the Gaussian width $\Delta f = \sqrt{2}n\bar{v}/L$ here is about 1.5 MHz, the flux produced by negative frequencies is expected to be small. Finally, note that both positive and negative fluxes are observed and that the flux peaks occur at different frequencies. This also seems to be qualitatively consistent with the theory. When the density gradient is large, the first term in the square brackets of Eq. (4) will dominate and we expect a bell-shaped curve, opposite in sign to dn_0/dr, centered around $\omega = l\omega_R$. This behavior is shown by the curves for r/R equal to 0.19, 0.30 and 0.52 . Note that in our experiment ω_R is set by the center wire bias ϕ_{cw} and decreases with radius

$$\omega_R = \frac{-c\phi_{cw}}{r^2 B_z \ln(R/a)} \tag{8}$$

and thus it is expected that the flux resonances will shift to lower frequencies with radius, as observed. Near the top of the density profile, the gradient is near zero, so the second term in the square brackets of Eq. (4) will dominate. We then expect an xe^{-x^2} behavior, consistent with the shape of the $r/R = 0.39$ curve.

To further check that the resonances are associated with ω_R, we have varied the center wire bias ϕ_{cw} and the axial magnetic field B_z. As expected, the flux resonances maintain their general shapes but shift to higher frequencies as the magnitude of ϕ_{cw} is increased and to lower frequencies as B_z is increased (see reference [19] for details).

As seen in Eq. (6), the theory also predicts a variation of f_{peak} with axial mode number n. To check this, we applied $n = 2$ and 3 asymmetries to the wall sectors. The results are shown in Fig. 3 along with data from the $n = 1$ configuration. Here we use an alternate method of displaying the frequency dependence of the flux: we plot the frequency at which the flux has an extremum, f_{peak}, versus radius. Data corresponding to both positive and negative flux peaks are shown. The points in the upper left portion of the graph give the frequencies of the negative flux peaks (flux minima) while the points in the lower right portion of the graph correspond to the positive flux peaks (flux maxima). The fall off of f_{peak} with radius is clear, as expected from the dependence of ω_R on r. The upward shift of f_{peak} with n is also clear, and the inset of the figure shows that f_{peak} increases linearly with n for three representative radii. The n-dependence of Eq. (6) is not simple (note that $B \propto n$), but deviates only slightly from linearity for experimental values of A/B and n ($-1 < nA/B < 2$). The observed n-dependence is thus consistent

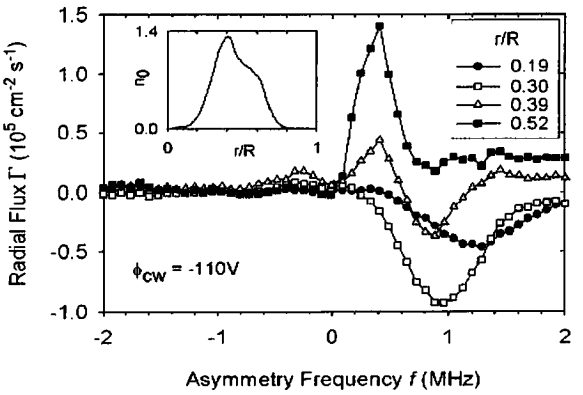

FIGURE 2. Radial particle flux at four selected radii as a function of asymmetry frequency for center wire bias ϕ_{cw} -110 V, magnetic field B =364 G, and Fourier mode numbers $n-1$, $l=1$. The shapes of the flux curves are qualitatively consistent with that expected from theory. Positive frequencies correspond to experiments where the asymmetry is rotating in the direction of the electron's azimuthal $E \times B$ drift and negative frequencies correspond to counter-drift rotations. The electron density n_0 (10^5 cm^{-3}) versus scaled radius r/R is shown in the inset.

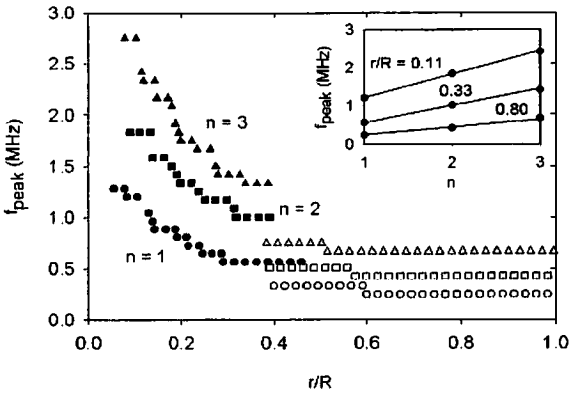

FIGURE 3. f_{peak} versus r for three values of the axial mode number n. The filled symbols in the upper left portion of the graph give the frequencies at which the flux is a minimum while the open symbols in the lower right portion of the graph correspond to frequencies of the flux maxima. A linear increase of f_{peak} with n is shown in the inset for three representative values of scaled radius r/R. Here, ϕ_{cw} = -146 V and B_z = 364 G.

with Eq. (6) for the flux minima data. For the flux maxima data, however, Eq. (6) predicts that f_{peak} will decrease with n, in contrast to the observed increase with n. Nevertheless, the dependence of f_{peak} on n shows that the transport we are studying depends on axial variation in the asymmetry, in contrast to earlier work on radial transport induced by $n = 0$ diocotron waves [20]. We have also verified that f_{peak} shifts upward appropriately for $l = 2$ asymmetries.

The dependence of f_{peak} on ϕ_{cw}, B_z, and r obeys an empirical scaling law, as shown in Fig. 4. Data with values of ϕ_{cw} from -20 V to -140 V and B_z values from 243 G to 607 G were scaled according to $f_{scaled} = f_{peak}\sqrt{\frac{B_z}{-\phi_{cw}}}$ and plotted versus r/R. The number of radial points plotted for each case was reduced for clarity. Although there is some scatter in the data, a fairly good universal curve is formed. The frequencies for the flux minima also scale inversely with the square root of the radius, as shown by the solid line. The scaling law for these points is thus

$$f_{peak}(\mathrm{MHz}) = \sqrt{\frac{-\phi_{cw}(\mathrm{V})}{B_z(\mathrm{G})}\frac{R}{r}}.$$

The frequencies for the flux maxima decrease slightly with radius, but the scatter in the data is too large to validate a particular radial dependence. If we ignore the radial variation, we obtain the rough scaling law

$$f_{peak}(\mathrm{MHz}) = 0.8\sqrt{\frac{-\phi_{cw}(\mathrm{V})}{B_z(\mathrm{G})}}.$$

As we have seen, the parametric dependence of f_{peak} on ϕ_{cw}, B_z, r, and, for the flux minima, n is qualitatively consistent with theory (i.e. f_{peak} increases and decrease appropriately). A quantitative comparison of experiment and theory, however, reveals serious discrepancies. To illustrate this, we have used experimental values to evaluate Eq. (6) and found f_{peak} as a function of radius r for the case where $n = 1, l = 1, B_z = 364$ G and ϕ_{cw} = -146 V. The results are shown in Fig. 5 along with the experimental data and the calculated f_R. While the experimental frequencies for the flux minima (solid circles) match the theory for $r/R \simeq 0.4$, they clearly diverge from theory at smaller radii. More seriously, the theory for these negative flux peaks constrains f_{peak} to be greater than the rotation frequency f_R, but the experimental data clearly crosses the f_R line, shown dotted in the figure. Flux minima data for $n = 2$ and 3 show similar behavior and a similar level of agreement. The data for the frequencies of the flux maxima (open circles) do not match the theory at any point. The theory for the positive flux peak shows f_{peak} going smoothly through zero to include negative values, while the experimental values always remain positive. Finally, as noted above, the theory has f_{peak} for the flux maxima decreasing with n, whereas the experiment shows an increase with n.

There are several simplifying assumptions made in the theory which might be involked to account for the discrepancy between theory and experiment. The theory used here assumes that the plasma particles specularly reflect at the ends of the trap and that this reflection point is the same at all radii (i.e. L is not a function of radius). The theory also assumes that the rotation frequency ω_R is not a function of axial position z. While these assumptions are clearly violated in our experiment, our estimates of these effects give corrections that are too small to account for the observed discrepancies.

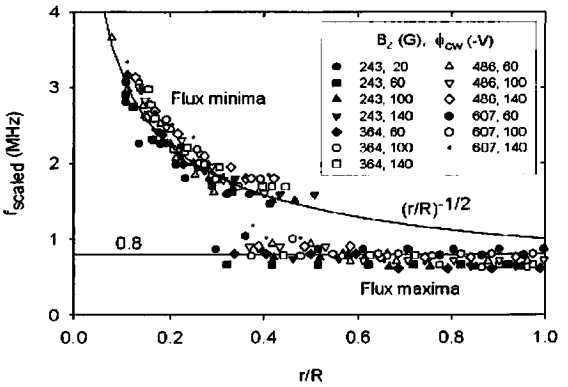

FIGURE 4. Empirical scaling of f_{peak}. Data having various values of B_z and ϕ_{cw} were scaled according to $f_{scaled} = f_{peak}\sqrt{\frac{B_z}{-\phi_{cw}}}$ and plotted versus the scaled radius r/R. Solid lines show simple "universal" curve fits to the resulting data points.

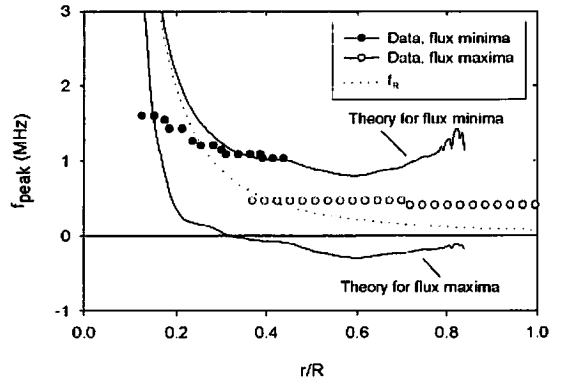

FIGURE 5. Comparison of experimental and theoretical values for f_{peak}. Experimental density profiles are used in Eq. (6) to produce the theory curves shown by the solid lines. Experimental data is also shown for this case, where B_z = 364 G and ϕ_{cw} = -146 V. The rotation frequency f_R is shown by the dotted line for comparison.

The theory used here also assumes that the plasma temperature T is constant with radius. A radial temperature variation would add a term $\frac{n_0}{T}\frac{dT}{dr}(x^2 - \frac{1}{2})$ to the square brackets of Eq. (4) and thus change the theoretical predictions for f_{peak}. Measurements of $T(r)$ in our experiment, however, show that this correction would also be too small to account for the discrepancies.

CONCLUSION

We have measured the frequency dependence of asymmetry-induced transport under very simple experimental conditions and compared the results to resonant particle theory. Our results are qualitatively consistent with the theory and support the idea that resonant particles dominate the transport, but the quantitative predictions of the simple theory employed here do not match the experiments. Apparently, the current theory does not give a complete description of this transport.

ACKNOWLEDGMENTS

This work was supported by U.S. Department of Energy grant No. DE-FG03-98ER54457. The contributions of Brenda Carrillo and Brian Fowler are gratefully acknowledged.

REFERENCES

1. C. F. Driscoll and J. H. Malmberg, Phys. Rev. Lett. **50**, 167 (1983).
2. C. F. Driscoll, K. S. Fine, and J. H. Malmberg, Phys. Fluids **29**, 2015 (1986).
3. D. L. Eggleston, T. M. O'Neil, and J. H. Malmberg, Phys. Rev. Lett. **53**, 982 (1984).
4. J. Notte and J. Fajans, Phys. Plasmas **1**, 1123 (1994).
5. X.-P. Huang, F. Anderegg, E. M. Hollman, C. F. Driscoll, and T. M. O'Neil, Phys. Rev. Lett. **78**, 875 (1997).
6. D. L. Eggleston, in *Non-Neutral Plasma Physics III*, edited by John J. Bollinger, Ross L. Spencer, and Ronald C. Davidson, (American Institute of Physics, Melville, NY, 1999), p. 241.
7. J. M. Kriesel and C. F. Driscoll, Phys. Rev. Lett. **85**, 2510 (2000).
8. D. L. Eggleston and B. Carrillo, Phys. Plasmas **9**, 786 (2002).
9. D. L. Eggleston, J. H. Malmberg, and T. M. O'Neil, Bull. Am. Phys. Soc. **30**, 1379 (1985).
10. E. Gilson and J. Fajans, in *Non-Neutral Plasma Physics IV*, edited by Francois Anderegg, C. Fred Driscoll, and Lutz Schweikhard, (American Institute of Physics, Melville, NY, 2002), p. 378.
11. D. Ryutov and G. Stupakov, Sov. J. Plasma Phys. **4**, 278 (1978).
12. R. Cohen, Comments Plasma Phys. Cont. Fusion **4**, 157 (1979).
13. D. L. Eggleston and T. M. O'Neil, Phys. Plasmas **6**, 2699 (1999).
14. J. H. Malmberg, C. F. Driscoll, B. Beck, D. L. Eggleston, J. Fajans, K. Fine, X.-P. Huang, and A. W. Hyatt in *Non-Neutral Plasma Physics*, edited by C. W. Roberson and C. F. Driscoll, (American Institute of Physics, Melville, NY, 1988), p. 28.
15. F. Anderegg, E.M. Hollmann, and C.F. Driscoll, Phys. Rev. Lett. **81**, 4875 (1998).
16. E.M. Hollmann, F. Anderegg, and C.F. Driscoll, Phys. Plasmas **7**, 2776 (2000).
17. D. L. Eggleston, Phys. Plasmas **4**, 1196 (1997).
18. D. L. Eggleston, Phys. Plasmas **1**, 3850 (1994).
19. D. L. Eggleston and B. Carrillo, Phys. Plasmas **10**, 1308 (2003).
20. J. S. DeGirassie and J. H. Malmberg, Phys. Rev. Lett. **39**, 1077 (1977).